# Thermal wave microscopy: fundamentals and applications

**S. Galovic[1,2], Z. Soskic[2], D. M. Todorovic[3]**

[1] The "Vinča" Institute of Nuclear Sciences, University of Belgrade, P. O. Box 522, 11001 Belgrade, Serbia
[2] Faculty of Mechanical Engineering Kraljevo, Department of Applied Mechanics, Mathematics and Physics, University of Kragujevac, Dositejeva 19, 36000 Kraljevo, Serbia
[3] Institute for Multidisciplinary Research, P. O. Box 33, 11030 Belgrade, Serbia

Thermal wave microscopy is used either for local characterization of materials and devices from the points of view of thermal and non-thermal (optical, elastic, electronic, etc.) properties, or for investigations of structures of opaque, semitransparent, and insulating samples. This chapter presents a review of various techniques of thermal wave microscopy and their application for testing of micro- and nano-structured materials and devices. The discussion of thermal wave microscopy research is divided into two main categories: 1) photoacoustic and photothermal microscopy and 2) scanning thermal microscopy. Within each category we describe the following: (a) the physical processes which generate thermal wave signal with emphasis on the unique capability for thermal wave visualization of the surface and subsurface structure of a sample; (b) the techniques developed for thermal wave detection; (c) the measurement characteristics such as spatiotemporal resolution, accuracy, sensitivity, and interpretation of measurement data, and (d) applications of the described thermal wave microscopy techniques. The review concludes by description of recent developments of application of scanning near-field optical microscopy and atomic force microscopy for thermal wave measurements, which might allow for higher spatial and time resolution measurements of various properties of substrates and thin films, as well as for sensing nanoscale targets and better understanding of thermal transfer at small scales in general.

**Keywords** photoacoustic microscopy; photothermal microscopy; scanning thermal microscopy; microscale heat transfer; thermoelastic microscopy, (micro)thermography

## 1. Introduction

Investigation of a structure, properties, and physical processes on small length and time (high frequency) scale becomes one of the most important tasks of various scientific areas, from physics, physical chemistry, and biology to optoelectronics, medicine and material science. Different aspects of low-dimension or very small spatial scale studies are nowadays joined in a modern scientific area called nanoscience. The trend of development of nanoscience was accompanied by design of novel microscopy techniques capable of appropriate (very high) spatial resolution (electron microscopes, focused ion beam microscopes, and scanning probe microscopes enable imaging of particular atoms [1,2]). Besides ultrahigh resolution in surface and subsurface imaging, the novel microscopy techniques should also be capable of characterization of physical properties, enabling composition analysis and understanding of interaction and transport processes that occur on submicron and nanometre scales and within short time intervals (for example, far-infrared microspectroscopy facilitates imaging and characterization of a sample with submicron resolution [3]). Among the modern-day microscopy methodologies, thermal wave (TW) detection is a technique with growing importance, due to its ability to monitor subsurface structures and damages in materials on the very small spatial scale, well beyond the penetration depth of photons or electrons, providing a new means for "at depth" imaging. Besides imaging, TW detection could enable determination of local properties of a sample.

TW microscopy is based on thermal excitation of either sample or probe by some external energy source, followed by detection of phenomena that is consequence of thermal waves propagation. TW undergo fairly large attenuation, and their range or depth of penetration is limited essentially to one or two thermal wavelengths. Direct detection of the TWs would thus be possible only for very thin samples. However, thermal wave techniques do not detect thermal waves directly. Instead, they are detected indirectly, through TW induced phenomena. Furthermore, by variation of the modulation frequency of energy source, and accompanying changes in the thermal waves' wavelength, depth-profile microscopic scanning can be performed.

There are two groups of TW microscopy techniques: on one side is photoacoustic (PA) and photothermal (PM) microscopy (PAM, PTM), while on the other side is scanning thermal microscopy (SThM). In the first group of microscopy techniques, the incident electromagnetic (optical) beam is used for generation of thermal waves in the sample. In the second group, some external energy source, optical or electrical, is used for heating of either sample or probe, and consequently, for generation of heat transfer between sample and tip. There are many types of the TW detection in both groups of TW microscopy techniques, offering possibility to select detection system most appropriate for the specific measurement request.

In the following two sections, the physical principles, methods of detection, performance characteristics, and applications of TW microscopies are considered. In the fourth section, the improvements of TW microscopies are discussed, both in the meaning of increasing resolution of microscopy and in the meaning of developing methods for reconstruction of thermal and thermoelastic properties of investigated samples.

 

## 2. Photoacoustic and photothermal microscopy

PAM and PTM consist basically of generation of localized periodic heating in a sample due to the absorption of an intensity-modulated energetic beam, and scanning of the heating position across the surface of the sample. The TWs resulting from the absorption of the modulated incident beam propagate from the heated regions, undergoing reflection and scattering when they encounter regions of different thermal and geometrical characteristics. In this way, as the heating beam is scanned across the sample, any surface or subsurface change in the thermal characteristics of the sample can be observed as a change in the TW induced signal. This change could be monitored either directly, as a variation of the temperature, or indirectly, as a variation of pressure or density [4-30].

PAM and PTM are typically used for local and non-destructive evaluation of materials and devices, as well as for studies of physical processes on micron scale. Their main advantage is their ability to detect and characterize types of flaws (material defects and interfaces) that are not visible optically or acoustically [7,9,10]. Examples of these kinds of defects include disbonds and poor adhesion in layered media, subsurface cracks or crystal damage in opaque solids, and electrical defects in active circuits.

### 2.1 Physical principles of PA and PT microscopy and thermal wave detection techniques

The underlying principle of PA and PT methods is detection of changes occuring in a sample due to heating produced by absorption of an incident energetic beam. The absorption and the subsequent non-radiative deexcitation-relaxation processes represent heat source in the sample, which may be distributed throughout its volume, or confined to its surface. This heat source gives rise to temperature, pressure, density, and free charge (if exists) fluctuations within the samples, which are then detected optically or by thermal or acoustic, or even both, sensing devices . In most cases, the heat deposited in the sample is due to the absorption of optical radiation and this is the reason for the name (photoacoustic and photothermal) of these techniques. Primary physical processes that occur during PA and PT characterization i.e., PA and PT microscopy are schematically depicted in Fig.1.

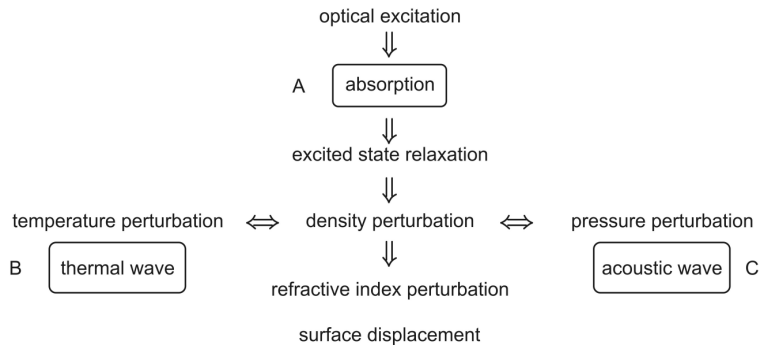


**Fig. 1**. Physical processes that occur during PAM and PTM.

Process A involves the absorption of the intensity-modulated incident energy, which can be either in the form of photons or particles such as electrons or ions. Process B involves the generation and propagation of the TWs that result from the energy absorption during process A and from subsequent generation of charge carriers. Finally, process C involves the generation and propagation of elastic waves that arise as a direct consequence of heating during process B.

Process A provides information about local absorption or reflection/scattering properties of the sample. If light is used as an energy source, then A is the same process that provides visualization in an optical microscope. If electrons, or other particles, are used as the incident energy beam, then process A is the same process that provides microscopic visualization in an electron or particle microscope. Obviously, the ultimate resolution of process A is determined by the wavelength of the photons or electrons (particles) [11]. Also, the depth of visualization is set by the penetration depth of the photons or electrons in a transmission microscope, or by the escape depth of the photons or electrons in a back-scattering microscope. Depth profiling, that is, visualization at selected and variable depth in the sample, is not readily possible with process A.

Process B is unique to TW microscopy, and does not occur in either optical (particle) or acoustic microscopy. This process provides information about local thermal properties such as thermal diffusivity, thermal memory properties, thermal conductivity, and the thermal expansion coefficient of the sample [4-30]. Visualization results from the interaction of the thermal waves with features in the sample that exhibit variation in thermal properties. The ultimate resolution in process B is determined by the wavelength of the thermal waves [5,11,12]. The thermal wavelength varies

with frequency $f$ at which the TW is generated. For most solids, the thermal wavelength, and thus the ultimate resolution, ranges from 30-300 $\mu m$ at $f$ = 100 Hz to 0.3-3 $\mu m$ at $f$ = 1 MHz.

Process C provides information about the local elastic properties of the sample. This is the same process that permits both surface and subsurface visualization in conventional ultrasonic flaw detectors and in acoustic microscopes. The ultimate resolution here is determined by the wavelength of the acoustic waves. For the most solids, it limits the ultimate resolution to 5-10 $\mu m$, even for acoustic microscopes operating at 1000 MHz. Higher resolutions are very difficult to achieve because of the excessive acoustic attenuation that occurs at these frequencies. Depth profiling is not possible in conventional transmission ultrasonics, although it can be performed in reflection mode using pulse-time techniques. Depth-profiling has apparently not been possible with acoustic microscopes.

In general, PA and PT microscopes will provide information about the sample from all three of the physical processes, A, B, and C, although in many cases one or more of these processes can be neglected. When process A dominates, the PA/PT image will be identical to that obtained with a conventional optical or electron microscope. When process C dominates, the image will be identical to that obtained with conventional ultrasonics or with an acoustic microscope. This will be true as long as the non-radiative or heating mode is primary deexcitation mechanism for the optically (or electron-) excited energy levels. The truly unique feature of a PA/PT microscope lies in its capability for providing surface and subsurface visualization through the interaction of thermal waves with sample

Processes A, B, and C produce the photothermal phenomena listed in Figure 2:

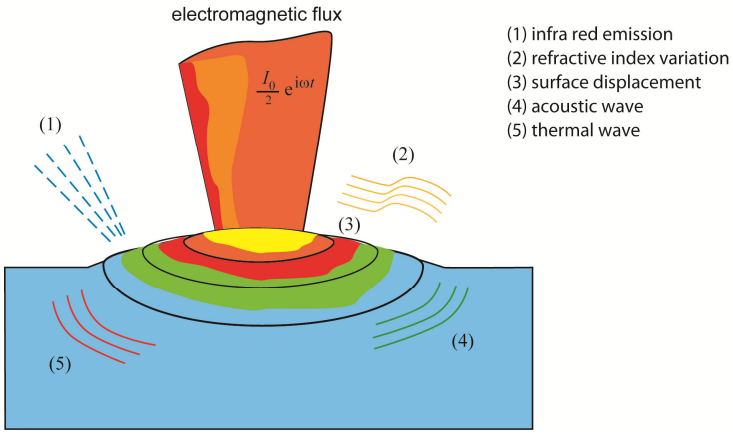


**Fig. 2** Photothermal phenomena which are consequence of optical heating of the sample

All this phenomena could be detected by appropriate detection techniques. There is a variety of methods used to monitor the thermal state of the sample [6,9,10] and the methods are summarized in Table 1.

**Table 1** Detection methods of PAM and PTM

| THERMODYNAMIC PARAMETER | MEASURED PROPERTY | DETECTION TECHNIQUE | |
|---|---|---|---|
| TEMPERATURE | TEMPERATURE<br>INFRARED EMISSION | PHOTOTHERMAL CALORIMETRY<br>PHOTOTHERMAL RADIOMETRY | |
| PRESSURE | ACOUSTIC WAVE | PHOTOACOUSTIC TECHNIQUES | |
| | SURFACE DEFORMATION | PHOTOACOUSTIC TECHNIQUES | OPTICAL DETECTION |
| DENSITY | REFRACTIVE INDEX | PHOTOTHERMAL LENS<br>PHOTOTHERMAL INTERFEROMETRY<br>PHOTOTHERMAL DEFLECTION<br>PHOTOTHERMAL REFRACTION<br>PHOTOTHERMAL DIFFRACTION | |
| | SURFACE DEFORMATION | SURFACE DEFLECTION | |

Temperature changes can be directly measured using thermocouples, thermistors, or pyroelectric devices by the PT calorimetry. These changes can also be indirectly measured using techniques which monitor infrared emission when the thermal infrared emission is related to the temperature of the sample [13,15]. Methods of thermal emission or PT radiometry of infrared radiation can be used to monitor relatively large temperature changes that occur as a consequence of optical absorption. Although not very sensitive, these methods have a great potential for application in non-destructive material evaluating and testing. Using infrared sensitive cameras, it can be used for imaging the thermal properties of large samples.

The changes in the two other temperature dependent thermodynamic parameters (see Table 1) which produce detectable PT phenomena (Fig.2) are also commonly exploited in indirect detection of thermal waves. If the temperature rise in the absorbing sample volum occurs faster than this volume can expand, a local pressure increase (acoustic wave) is the consequence. The pressure changes that occur upon periodic or pulsed sample heating can be detected by microphones or other pressure transducers, in order to monitor the acoustic wave. Acoustic waves are also generated within the sample itself by thermoelastic effects in region where the energy is absorbed from the heating incident beam. The thermoelastic fluctuations can be observed through surface displacement by optical methods [30]. In the both cases, detection method is called photoacoustic.

The PT methods refer to methods that monitor the temperature dependent refractive index changes, usually with a probe laser (see Table 1). In transparent samples, the temperature dependent refractive index of the sample itself is probed. For opaque or scattering surfaces, temperature dependent changes in the refractive index of fluid that conducts heat out of a solid sample are measured. There are several methods used to detect the resulting refractive index change: PT lens, PT interferometry, PT deflection, PT modulation refractometry, and PT diffraction. All of these methods rely on a few basic principles of light propagation: optical pathlength changes, diffraction and refraction. Light refraction can result in a direction change and/or focusing. The optical pathlength changes that occur due to the PT induced refractive index changes can be measured by various optical interferometric techniques. Using interferometry, the phase of monochromatic light passing through the heated sample, relative to the phase passing through the reference arm, results in a change in power at a photoelectric detector. There are several different interferometric schemes that can be used to detect changes in the optical pathlength. These methods may be classified as PT interferometry. Spatial gradients of refractive index result in a direction changes in the propagation of a ray of light. Thus, light will exit a medium with a refractive index gradient at an angle relative to the incident ray. This bending of light path is commonly called PT deflection method. Spatial dependent refractive index profiles can also result in focusing or defocusing of light. This occurs when the refractive index profiles are curved. Thus the thermally perturbed sample can act as a thermal lens. Light transmitted through an aperture placed beyond the PT lens will vary with the strength of the lens. PT methods based on measurement of the strength of this lens are called the thermal lens methods. Some experimental apparatuses measure a signal that is due to the combined effects of deflection and lensing. These may be generally classified as PT refraction methods. At last, a periodic spatial refractive index modulation results in a volume phase diffraction grating. The grating will diffract light at an angle that meets requirements from Bragg's Law. The amount of light diffracted is proportional to the refractive index change. The diffracted light is measured with photoelectric detector. Methods used to measure spectroscopic signals based on volume phase diffraction gratings formed by the photothermal effects are called PT diffraction methods.

Under steady-state and isobaric conditions, the density thorough the sample is related to the temperature through the volume expansion coefficient. Temperature dependent density changes are difficult to measure directly. But density changes can affect samples in several different ways. In solid samples, the density changes alter physical dimensions at sample surfaces. Sample dimension changes give rise to two optical methods for monitoring the temperature change based on surface deformation. A homogeneous deformation (expansion or contraction) displaces the surface of the sample. Interferometry can be used on refractive samples. Since small displacements, of the order of a few parts-per-million of the wavelength of probe beam light, can be measured using the optical interferometer, this method may be used for sensitive measurements of solid sample absorption. Spatially heterogeneous expansion (or contraction) can also cause the surface angle to change. A probe beam reflected from the surface will change angle when heterogeneous expansion occurs. Measurement of the probe beam angle leads to the PT surface deflection method.

### 2.2 Performances and applications of PA and PT microscopy

There are certain experimental advantages of PA/PT microscopy: existence of the several complementary detection schemes; the fact that the technique is specific to the near subsurface region, with a controllable depth range; high resolution (~1 $\mu m$ ) capability; and the adaptability of the technique to specimens of complex geometry.

The classical PA/PT microscopies are diffraction-limited techniques because of far-field detection [11]. The spatial resolution of these techniques is limited to a theoretical spatial resolution of

$$d = \frac{\lambda_1}{NA} \quad (1)$$

where $\lambda_1$ is the wavelength of light and $NA$ is the numerical aperture of the used lens. The highest numerical aperture

that can be achieved is about 1.6, and, hence, the best spatial resolution is ~ 1 $\mu m$ .

The vertical spatial resolution of PA/PT microscopy techniques is determined by the wavelength of thermal wave and consequently by modulation frequency of incident energetic beam, $f$ [5]:

$$\lambda_{th} = \sqrt{\frac{2D_T}{2\pi f\sqrt{1+(2\pi f)^2\tau_s^2}+(2\pi f)^2\tau_s}} \quad (2)$$

$D_T$ represents thermal diffusion length and $\tau_s$ thermal relaxation time.

The depth of sample z up to which PMA/PTM are applicable, is determined by diffusion length of thermal wave. This length depends on frequency $f$ of generated waves (it is the modulation frequency of the light source) in the following way [5]:

$$z = \sqrt{\frac{2D_T}{2\pi f\sqrt{1+(2\pi f)^2\tau_s^2}-(2\pi f)^2\tau_s}} \quad (3)$$

Increase of the modulation frequency leads to a decrease of the penetration depth, as it could be seen from Equation (3). It means that the sample depth which could be imaged decreases with increase of modulation frequency, but the vertical resolution increases, (Eq. 2). The minimal depth which can be imaged is

$$z_{\min} = 2\sqrt{D_T\tau_S} \quad (4)$$

and depends on thermal properties of the imaged sample.

An attractive feature of PA/PT microscopy is the simplicity of theoretical interpretation of thermal wave image. This arises from the following facts: only a single scalar parameter, the temperature, is needed to describe the wave; the wave is very highly damped, minimizing problems of multiple scattering and resonance; it is easy to obtain experimental phase information about the scattered waves. The mathematical model of a direct PA/PT problem is given by the following set of partial differential equation (direct PA/PT problem) [14,17-20]:

$$\frac{\partial\Delta n(\vec{r},t)}{\partial t} = D_E\nabla^2\Delta n(\vec{r},t) - \frac{\Delta n(\vec{r},t)}{\tau_E} + \frac{\partial\Delta n(\vec{r},t)}{\partial t}\frac{\partial T(\vec{r},t)}{\tau_E} + Q(\vec{r},t) \quad (5)$$

$$\rho C\left[\frac{\partial T(\vec{r},t)}{\partial t} + \tau_s\frac{\partial^2 T(\vec{r},t)}{\partial t^2}\right] = k\nabla^2 T(\vec{r},t) + \frac{E_g}{\tau_E}\Delta n(\vec{r},t) + \beta_u\rho C\,\nabla^2\frac{\partial\vec{u}(\vec{r},t)}{\partial t} + H(\vec{r},t) \quad (6)$$

$$\rho\frac{\partial^2\vec{u}(\vec{r},t)}{\partial t^2} = \mu\nabla^2\vec{u}(\vec{r},t) + (\lambda+\mu)\nabla\left[\nabla\times\vec{u}(\vec{r},t)\right] - \beta_T\nabla T(\vec{r},t) - d_n\nabla\Delta n(\vec{r},t) \quad (7)$$

where $\Delta n(\vec{r},t)$ stands for excess of carrier density, $T(\vec{r},t)$ for temperature distribution, $\vec{u}(\vec{r},t)$ for elastic displacement, $D_E$ for coefficient of ambipolar diffusion of carriers, $\tau_E$ for lifetime of photogenerated carriers, $\rho$ for density, $C$ for thermal capacity, $k$ for thermal conductivity, $E_g$ for energy gap, $\beta_u$ for coupling between plasma and thermal waves, $\mu$ for shear modulus, $\lambda$ for Lames constant, $\beta_T = (3\lambda+2\mu)\alpha_T$ for coefficient of thermoelastic coupling, $\alpha_T$ for coefficient of linear thermal expansion, $d_n$ for coefficient of electronic deformation, $Q(\vec{r},t)$ for carrier photogeneration source term, and $H(\vec{r},t)$ for optically generated thermal sources.

In most practical cases, the coupling between plasma and thermal waves can be neglected [14,17-20]. So the plasma wave and thermal wave solutions can be obtained via solving the two isolated equations (5) and (6). The solution of direct problem is used in design of PAM and PTM, as well as in evaluation of the inverse PA/PT problem, and thermal image reconstruction [21-23].

In order to enable thermal imaging, many algorithms for reconstruction of image have been developed. The most famous algorithm is known as the universal back projection algorithm [24]. This method is suitable for three imaging geometries: planar, spherical, and cylindrical. In the same time, many techniques of solving of inverse PA/PT problems have been developed which enable local characterization of thermoelastic and plasmaelastic properties of a sample.

Many authors have described PA imaging and microscopy [25-30]. Peltz et. al. have given an overview on the application of thermal wave methods and discussed the application of PT beam deflection for position sensitive spectroscopic methods on inorganic crystals. Aamdot et. al. were first to use a localized excitation and investigate cracks [25]. Walther et. al. have developed a photothermal mirage interferometer for imaging of hidden structures [26]. With PT displacement inspection carried out by Welsh et. al. it was possible to achieve micrometer resolution of thin optical coatings of inorganic materials. Kreiter et al. used localized excitation and scanning technique to image absorption-and therefore, by Kramers-Kronig relations, refractive index-pattern in polymeric materials by mirage effect and by the thermal displacement for inspection of polymeric integrated optical devices [27]. Grice et. al. have used photoacoustic and mirage effects to image closed cracks in solids [28], and McDonald an co-worker have used the mirage effect to investigate vertical interfaces, both at macroscopic scale [29]. Boccara and a co-worker have used PT microscope to investigate thermal barriers at the grain boundaries in ceramic materials and thin films of alumina.

 

Recently, PAM has been developed for biomedical applications [30]. Some of examples are detection of changes in oxygenated/deoxygenated haemoglobin in small vessels, in vivo imaging of skin melanoma, visualization of blood vessels, tumor angiogenesis monitoring, blood oxygenation mapping, functional brain imaging, etc.

## 3. Scanning thermal microscopy

Scanning thermal microscopy (SThM) is a type of scanning probe microscopy that maps the local temperature and thermal, optical or some other physical or chemical properties of an interface. There are various techniques of SThM, but all of them use temperature-sensing probes together with the scanner and probe control (feedback) system similar as in scanning tunnel microscopes or atomic force microscopes. The probe in a scanning thermal microscope enables creation of the nanoscale thermometer. Thermal measurements at the nanometre scale are of both scientific and industrial interest. These measurements include: local surface temperature, thermal properties of materials, glass transition, latent heat, enthalpy, but also optical absorbance, contact potential, surface topography, subsurface imaging, etc. [31-45].

### 3.1 Physical principles of SThM and detection techniques

The physical principle, on which the most of SThM techniques are based, is the induction of heat transfer between the sample and the tip, and detection of the effects produced by it. Heat transfer could be induced either by heating of the probe or by heating of the sample. The probe and the sample could be heated either optically (PT effect) or electrically.

There are several mechanisms of the tip-sample heat transfer. These are: solid-solid heat conduction, conduction by the surrounding gas, near-field radiation and conduction through a liquid film that forms owing to capillary condensation that bridges the tip and the sample. Practically, some of mentioned mechanisms are not significant. Only dominant mechanisms affect spatial resolution and sensitivity of SThM measurement. The influence of particular mechanism is theoretically estimated by its thermal conductance, and experimentally, based on thermal contrast that is obtained in specially defined measurement which excludes some of the mechanisms (for example, the measurement in vacuum exclude conduction by surrounding gas, or measurement in noncontact mode excludes solid-solid heat conduction).

The theoretical explanation of tip-sample heat transfer processes is very important for engineering of a thermal probe in order to obtain ultrahigh spatial and temperature resolution as well as for relating the sample properties to measured thermal contrast image enabling composition and/or properties analysis by SThM. Considering that lateral dimension of temperature sensor is about 10 $\mu m$, contact spot size that ranges 3-10 nm, the distance between a tip and investigated sample surface that is about 5 nm, and order of magnitude of modulation frequency is about 100 MHz (i.e. order of time interval of heat transfer about 10 ns) it is easy to conclude that thermal transport processes in SThM are occur on small spatial and time scales. That processes are not theoretically explained yet [46-49]. It is very attractive area of investigation in the physics of condensed matter. The approximate theoretical and experimental diagnosis of these processes to performance of influence SThM has been made in [31] and references mentioned therein. In this section, in Table 2, the systematic review of the results of previous theoretical and experimental investigations is given.

**Table 2** Effective conductances and experimentally observed influence of tip-sample heat transfer mechanisms.

| mechanism | solid-solid | Gas | near-field radiation | liquid-film conduction |
|---|---|---|---|---|
| theoretically estimated conductance [W/K] | $10^{-8}$-$10^{-6}$ | $10^{-7}$-$10^{-6}$ | $10^{-13}$-$10^{-9}$ | $10^{-5}$ |
| experimental observation | insignificant | very significant | significant under ultra-high vacuum | dominate mode |

As it could be seen from Table 2, the experimentally observed influence of different mechanisms of heat transfer is not in agreement with the theoretical estimations of effective conductances of tip-sample-surroundings systems. It indicates drawbacks of theory. Experimental results, which already were used in design of thermal probes for ultrahigh spatial resolution, could be used in development of theory of heat transfer on nanoscale, and consequently, in design of SThM techniques with higher resolution.

Heat transfer between the tip and the sample is monitored by three different kinds of measurements, dependent on the probe type. If the tip is a temperature sensor, than heat transfer effects could be detected by thermovoltage-based

measurement, or by electrical resistance techniques. If the whole probe is temperature sensor, for example, a temperature-sensing tip on a bimaterial cantilever, than thermal expansion measurements are used.

There are two types of thermal sensor tips: thermocouple probes where the probe temperature is monitored by a thermocouple junction at the probe tip and resistive or bolometer probes where the probe temperature is monitored by a thin film resistor at probe tip. In a bolometer probe the resistor is used as a local heater and the fractional change in probe resistance is used to detect the temperature and/or the thermal conductance of the sample. As the probe is scanned, the amount of heat flow between the tip and the sample is changed in dependence on the tip-sample distance or on the local thermal properties of the sample. By monitoring the heat flow, a surface topography or thermal map of the sample could be created.

In the third type of detection, thermal expansion measurement, the whole cantilever is used as a temperature sensor. If a bimaterial cantilever is formed, temperature sensing tip induces a bending moment due to mismatch in thermal expansion coefficient of two cantilever materials, which results in a cantilever deflection. The measurement of deflection is, therefore, a measurement of temperature. Several issues need to be addressed concerning this technique. First, the probe must be designed to provide the maximum deflection. The second issue that turns out to be very important is that of tip-sample heat transfer. To be able to perform thermal microscopy, it is desirable that most of the heat flows through the tip. Under ambient conditions, the conduction through the surrounding gas dominates the heat transfer from the sample to the cantilever. Hence, the experiment must be operated in a vacuum, or the probe must be designed such that the heat flow through the tip is enhanced. This remains one of the main drawbacks of the technique.

The mode of detection of tip-sample heat transfer determines temperature and time resolution of SThM, and it will be discussed in the following subsection.

### 3.2 Performances and applications of SThM

The most important performances of SThM are temperature, time, and spatial resolution. Temperature and time resolution are determined by type of temperature sensor and detection chain of SThM, while the diameter of thermal probe determines the spatial resolution, as it is the case with all near-field microscopy techniques.

The thermal noise $\Delta T_{noise}$ limit for thermocouple measurements can be estimated by the relation

$$\rho_{noise} = \frac{\sqrt{4k_B TR}}{S}, \quad \Delta T_{noise} = \rho_{noise}\sqrt{\Delta f} \quad (8)$$

where $\rho_{noise}$ is noise density of the thermal noise which has a flat white-noise spectrum (this holds for frequencies typically higher than ~300-500 Hz, and a system is often modulated at frequencies higher than 500 Hz so that the measurement noise is reduced), $k_B$ is the Boltzmann constant, $T$ is the absolute temperature, $R$ is the electrical resistance of the thermocouple junction and wires, $S$ is the thermopower of the junction, and $\Delta f$ is the frequency bandwidth of measurements. This limit determines the temperature resolution of a thermocouple, i.e. its ability to distinguish a change in temperature.

As it could be seen from Equation (7), the temperature resolution can be increased by several means: reducing the bandwidth $\Delta f$ by lock-in techniques, reducing the electrical resistance $R$, or increasing the thermopower $S$ by choosing appropriate materials. At room temperature, the resolution that thermocouples can be obtained is typically ~$10^{-3}$K.

In the case of thermal expansion detection, the measurement of deflection is a measurement of temperature. Because the optical detection scheme in an AFM has a resolution of ~0.01 nm, this relates to a temperature resolution of $10^{-5}$K, which is far better than that of a thermocouple or a bolometer.

The temporal resolution of a temperature sensor is determined by the largest of time constants: external $\tau_{ext}$, internal $\tau_{\text{int}}$, or the averaging time $\tau_{LI}$ of the lock-in amplifier. The external and internal time constants could be estimated by the following relations:

$$\tau_{ext} = (mC)R_{ext} \quad \tau_{\text{int}} = l^2 / D_T \quad (9)$$

where $mC$ is the thermal mass of the sensor, $R_{ext}$ is the external thermal resistance, $l$ is the characteristic size of the system, and $D_T$ is the thermal diffusivity of tip material.

Usually, the limiting time constant is not one that of the system sensor-surrounding gas but that of the averaging time $\tau_{LI}$ of the lock-in amplifier, which is related to bandwidth through the relation

$$\tau_{LI} = \frac{1}{2\pi\,\Delta f} \quad (10)$$

As it could be concluded from Equations (8) and (10), reduction of bandwidth reduces noise and increases temperature resolution, but it also reduces the time resolution. Typical time resolution of SThM limited by $\tau_{LI}$ are ~50 ms, and time resolution limited by external and internal time constants are ~ 0.1-0.3 ms and 10 ns, respectively.

 

The space resolution which is attainable by SThM is determined by the dominant mechanism of the tip-sample heat transfer, although thermal noise may sometimes be limiting factor. If it is the case, the spatial resolution may be estimated on the basis of the following relation:

$$\Delta x = \frac{\Delta T_{noise}}{(dT/dx)_{measured}} \quad (11)$$

where $dT/dx$ is the measured temperature gradient on the sample. The noise-equivalent spatial resolution is of the order of 10-20 nm [35].

The spatial resolution is at most of the order of tip diameter or tip-sample contact size if conduction by the surrounding gas can be neglected. The maximal spatial resolution of SThM, depending on the probe diameter, probe design and manufacturing, is 30nm-15 $\mu m$. If the gas conduction has a dominant role in tip-sample heat transfer, the mean free path of gas layer $l_{mfp}$ is a characteristic length scale. From kinetic theory this is

$$l_{mfp} = \frac{k_b T}{p\sigma} \quad (12)$$

where $p$ is the pressure and $\sigma$ is the collision cross-section of a gas molecule. The mean free path of air at atmospheric pressure, $l_{mfp}$ is ~0.2-0.3 $\mu m$. Being that it is the average distance that gas molecules travel before they transfer their energy, the spatial resolution cannot be better than this length scale. An increase in pressure should decrease the mean free path and could improve the spatial resolution. In the limit of gas condensation and liquid formation, the mean free path in the liquid can be on the order of atomic distances, 0.1-1 nm. Hence, use of liquids could also improve the spatial resolution.

In the case of tunnelling thermocouple, a spatial resolution of ~ 1nm was observed. This is substantially better than the thermal diffusion length within the sample [33,34]. It must be noted that the length scale over which temperature can be defined is the mean free path of energy carriers. In metals at room temperature, this is ~10nm, which is the mean free path of inelastic electrons at the Fermi level. The fact that measurements were made over a spatial resolution of 1 nm suggests that although the tip and sample may have been under equilibrium, non-equlibrium conditions may have occurred in the sample around the tunnel junction. Hence, the contrast mechanism in this imaging technique may not have been only thermal in origin but possibly caused by the local changes in optical absorption or electron scattering.

The primary purpose of the original SThM was not to measure surface temperatures or thermal properties of a sample but for imaging insulating surfaces-something that scanning tunnelling microscopy (STM) and atomic force microscopy (AFM) were unable to do. However, potential for application of SThM for much wider range of application was soon recognized.. Developmnt of various thermal probes leads to enhanced performances, but also to widening of range of applications. So far, SThM was used for high resolution topography, subsurface defect imaging and thermal imaging of microelectronic and optoelectronic devices [35-42], for measurements of optical absorption with nanometre-scale spatial resolution, for contact potential measurement, for studying of radiative heating and absorption spectroscopy of metals [38], etc. Many groups have used the electrical resistance probes for thermal imaging, property measurement, and localized calorimetry [3,43] of different types of polymer blends.

Despite the successful use of SThM techniques for surface topography and imaging of thermal properties, optical absorbance, contact potential, etc. with very high spatial resolution, a thorough analysis of the signal is still missing. To understand how the signals depend on the local thermal properties of the sample, it is necessary to develop a complex model based on better knowledge of nanoscale heat transfer processes.

## 4. Recent and future development of TW microscopy

One of the most important tasks in TW microscopy is increase of spatial resolution. The state-of-the-art is given in Table 3.

**Table 3** Resolution of various TW microscopy techniques

| Techniques | | spatial resolution |
|---|---|---|
| infrared thermometry (PTM) | far-field detection | 1-10 $\mu m$ |
| laser surface reflectance (PTM) | | 1 $\mu m$ |
| Raman microspectroscopy | | 1 $\mu m$ |
| near-field optical thermometry | | < 1 $\mu m$ |
| scanning thermal microscopy | | < 100 nm |

Far-field microscopy techniques, such as classical PAM or PTM have been developed and used successfully for measuring various spatial distributions (temperature distribution, thermoelastic, optical and other properties of electronic devices, biological tissues, etc.) on micrometer scale as it is discussed in Section 2. These techniques are diffraction limited in their spatial resolution to ~ 1 $\mu m$ (see Table 2). Although it is possible to use ultraviolet light to increase the spatial resolution to about 100 nm, imaging below 100 nm requires an entirely different approach. On the other hand, due to the race toward miniaturization (for example in semiconductor technology), the experimental devices which are able to investigate thermal phenomena on the scale below 100 nm have to be developed.

It has been shown in Section 3 that many techniques have been developed in order to characterize the local thermal properties on sub-micrometer scale (see Table 2). All these techniques are derived from the two main families of near-field microscopes, STM and AFM. The study presented in this section is given as a supplement to the method reviewed. The overcoming of diffraction limit and increase of spatial resolution could be accomplished by scanning near-field optical microscopy (SNOM) techniques. The SNOM involves stretched optical fibre, which can be metalized at the tip end and have a small aperture. The excitation laser beam is injected into optical fibre and locally heats the fibre extremity and the sample. The high power density at the tip end is a heat source and thermal effects could be detected in all SNOM which use a metalized fibre tip. One interesting realization of near-field PTM has been presented in [11]. There is used another laser beam, of different wavelength as probe beam. The pump beam and probe beam are superimposed inside a fibre, and small part of each reaches the surface of the sample and they interact there. The probe laser beam is used to detect both apparent optical reflectance and dynamic PT signal. The estimated spatial resolution was about 80 nm.

To improve the spatial resolution in SThM, it is necessary to make the tip sharp, as it could be concluded from discussion in Section 3. However, increase in tip sharpness comes at the increased cost of reduction in tip-sample heat transfer. One would ideally like to develop a technique that does not rely on tip-sample heat transfer and yet measures the temperature distribution of the sample. One such technique, called scanning joule expansion microscopy (SJEM), has been recently developed [42]. An AFM is used to bring a sharp tip into force-controlled contact with the sample surface and to perform a raster scan. A sinusoidal or pulsed voltage produces sample joule heating and a temperature rise, resulting in sample thermal expansion. The AFM photodiode detects the cantilever deflection due to both sample thermal expansion and sample topography. The lock-in amplifier is tuned to the joule heating frequency, which detect only the expansion signal and provides this to an auxiliary AFM channel to form the expansion image. The advantage of the SJEM is that it eliminates the need to fabricate a sensor on the probe tip, and, therefore, commercially available probes can be used. Because it does not rely on tip-sample heat transfer, the performance of the technique improves with tip sharpness since it does not draw from or supply any energy to the sample. Because SJEM requires measurement of cantilever vibration at sufficiently high frequencies, it is very important to understand the dynamics of cantilever [14,17]. This topic requires further in-depth study.

Imaging has been the main goal of microscopists, but the interaction at the local scale is often complicated, and now the main question is how to understand the origin of the contrast in the obtained image and how to quantify the physical properties of the investigated systems. No complete answer can be given now, and it is one of the main directions in recent development of TW microscopy.

**Acknowledgements** This work is supported by Ministry of Science and Technological Development of the Republic of Serbia (Projects TR11027, 141013, and I.T.1.04.0062.B).

## References

[1] Giessibl FJ. Advances in atomic force microscopy. *Reviews of Modern Physics.* 2003;75: 949
[2] Chen CJ. *Introduction to Scanning Tunnelling Microscopy.* 2nd ed. Oxford, Md: Oxford University Press; 2008.
[3] Hammiche A, Bozec L, German MJ, Chalmers JM, Everall NJ, Poulter G, Reding M, Grandy DB, Martin FL, and Pollock MH. Mid-infrared Microspectroscopy of Difficult Samples Using Near-Field Photothermal Microspectroscopy. *Spectroscopy.* 2004;19:20-38.
[4] Thomas RL and Favro LD. From Photoacoustic Microscopy to Thermal Wave Imaging. *MRS Bulletin*. 1996;47-52.
[5] Galovic S, Kostoski D.Photothermal wave propagation in media with thermal memory. *J. Appl.Phys.* 2003;95:2063-2070.
[6] Vargas H and Miranda LCM. Photoacoustic and related photothermal techniques. *Physics Reports.* 1998;161:45-101.
[7] Rosencwaig A. Thermal wave microscopy with photoacoustics. *J. Appl. Phys.* 1980;51:2210-2211.
[8] Fournier D, Forget BC, Boue C, Roger JP. Micron scale photothermal imaging. *Int. J. Therm. Sci.* 2000;39:514-518.
[9] Bialkowski SE. *Photothermal Spectroscopy Methods for Chemical Analysis*. John Wiley&Sons, Inc. 1996.
[10] Terasina M, Hirota N, Braslavsky SE, Mandelis A, Bialkowski SE, Diebold GJ, Miller RSD, Fournier D, Palmer RA, and Tam A. Quantities, terminology, and symbols in photothermal and related spectroscopies. *Pure Appl. Chem.* 2004;76:1083-1118
[11] Cretin B. Scanning near-field thermal and thermoacoustic microscopy: performances and limitations. *Superlattices and Microstructures.* 2004;35:253-268.
[12] Galovic S, Stojanovic Z, Cevizovic D, Popovic M. Photothermal microscopy: a step from thermal wave visualization to spatially localized thermal analysis. *Journal of Microscopy.* 2008;232:558-561.

 

[13] Ippolito SB, Thorne SA, Eraslan MG, Goldberg BB, and Unlu MS. High spatial resolution subsurface thermal emission microscopy. *Appl. Phys. Lett.* 2004;84:4529-4531.
[14] Song Y, Cretin B, Todorovic DM, and Vairac P. Study of photothermal vibrations of semiconductor cantilevers near the resonant frequency. *J. Phys. D:Appl.Phys.* 2008;41:155106.
[15] Wu D, Busse G. Lock-in thermography for nondestructive evaluation of materials. *Rev. Gen. Therm.* 1998;37:693-703.
[16] Pottier L. Micrometer scale visualization of thermal waves by photoreflectance microscopy. *Appl. Phys. Lett.* 1994;64:1618-1619.
[17] Todorovic DM, Cretin B, Song YQ, and Vairac P. Electronic and thermal generation of vibrations of optically excited cantilevers *J. Appl. Phys.* 2010;107:023516-023525.
[18] Todorovic DM. Plasma, thermal and elastic waves in semiconductor. *Rev. Sci. Inst.* 2003;74:582-585.
[19] Todorovic DM. Plasmaelastic and thermoelastic waves in semiconductor. *J.Phys IV Francet.* 2005;125:551-555.
[20] Song Y, Todorovic DM, Cretin B, Vairac P.Study on the generalized thermoelastic vibration of the optically excited semiconducting microcantilever. *Int. J. Solids Struct.*. 2010;47:1871-1875.
[21] Galovic S, Soskic Z, Popovic M. Reconstruction of the optical depth structure from photothermal response. *to be published*
[22] Galovic S, Soskic Z, Popovic M. Analysis of photothermal response of thin solid films by analogy with passive linear electric networks. *Thermal Science*. 2009;13:129-142
[23] Power JF. Inverse problem theory in the optical depth profilometry of thin films. *Rev. Sci. Inst.* 2002;73:4057-4141
[24] Xu M, Wang LV. Universal back projection algorithm for photoacoustic computed tomography. *Phys. Rev. E*. 2005; 71;016706
[25] Aamdot LC, Murphy JC. Photothermal measurement using localized excitation source. *J. Appl.Phys.* 1981;52:4903.
[26] Walther HG, Freidrich K, Goring R, Haupt K, Seidel U. *Photoacoustic and Photothermal Phenomena III: Series in Optical Sciences Bd*, Berlin, Springer, 1992.
[27] Kreiter MJS, Mittler-Neher S. Scanning photothermal beam deflection and scanning photothermal displacement imaging of polymer channel waveguides: a comparison. *Thin Solid Films.* 1999;342:244-248
[28] Grice KR, Inglehart LJ, Favro LD, Kuo PK, Thomas RL. Thermal wave imaging of closed cracks in opaque solids *J. Appl. Phys.* 1983;54:6245
[29] McDonald FA, Westel GC Jr, Jamieson GE. Photothermal beam-deflection imaging of vertical interfaces in solids. *Can. J. Phys.* 1986;64:1265.
[30] Xu M, Wang LH. Photoacoustic imaging in biomedicine. *Rev. Sci. Instrum.* 2006; 77: 041101.
[31] Majumdar A. Scanning thermal microscopy. *Annu. Rev. Mater. Sci.* 1999;29:505-585.
[32] Cretin B, Patois R., Serio B. Near-field thermoelastic imaging coupled with infrared detection. *Superlattices and Microstructures.* 2004;35:297-304
[33] Stopka M, Oesterschulze E, Schulte J, and Kassing R. Photothermal scanning near-field microscopy. *Material Science and Engineering.* 1994;B24:226-228.
[34] Leavens CR, Aers GC. Vacuum tunneling thermopower: Normal metal electrodes. *Solid State Commun.* 1987;61:289-295.
[35] Marchall J, Majumdar A. *J. Appl. Phys*. 1993;74:168-170
[36] Majumdar A., Lai J, Chandrachood M, Nakabeppu O, Wu J, Shi J. Thermal imaging by atomic force microscopy using termocouple cantilever probes. *Rev. Sci. Instrum.* 1995;66:3584-3592.
[37] Oestershulze E, Stopka M, Ackermann L, Scholz W, Werner S. Thermal imaging of thin films by scanning thermal microscope. *J. Vac. Sci. Technol. B*. 1996;14:832-837.
[38] Hammiche A, Hourston DJ, Pollock HM, Reading M., and Song M. Scanning thermal microscopy: Subsurface imaging, thermal mapping of polymer blends, and localized calorimetry. *J. Vac. Sci. Technol. B*. 1996;14:1486.
[39] Stopka M, Hadjiiski L, Oestershulze E. Surface investigations by scanning thermal microscopy. *J. Vac. Sci. Technol. B*. 1995;13:2153-2156.
[40] Luo K, Shi Z, Varesi J, Majumdar A. Sensor nanofabrication, performance, and conduction mechanisms in scanning thermal microscopy. *J. Vac. Sci. Technol. B*. 1997;15:349-360.
[41] Luo K, Herrick RW, Majumdar A, Petroff P. Scanning thermal microscopy of a vertical-cavity surface-emitting laser. *Appl. Phys. Lett.* 1997;71:1604-1606.
[42] Nakabeppu O, Chandrachood M, Wu Y, Lai L, Majumdar J. Scanning thermal imaging microscopy using composite cantilever probe. *Appl. Phys. Lett.* 1995;66:694-696.
[43] Nonnenmacher M, Wickramasinghe HK. Optical absorption spectroscopy by scanning force microscopy. *Ultramicroscopy*. 1992;42-44:351-354.
[44] Xu JB, Wilson IH. Heat transfer between two metallic surfaces at small distances. *J. Appl. Phys.* 1994;76:7209-7216.
[45] Hammiche A, Reading M, Pollock HM, Song M, Hourston DJ. Localized thermal analysis using a miniaturized resistive probe. *Rev. Sci. Instrum.* 1996;67:4268-4274.
[46] Varesi J, Majumdar A. Scanning Joule expansion microscopy at nanometer scales. *Appl. Phys. Lett.* 1998;72:37-39.
[47] Cahill DG, Ford WK, Goodson KE, Mahan GD, Majumdar A, Maris HJ, Merlin R, Phillpot SR. Nanoscale thermal transport. *J. Appl.Phys.* 2003;93:793-818.
[48] Rego LGC. Thermal Transport in the Quantum Regime. *Phys. Stat. Sol. (a)*. 2001;187:239-251
[49] Chen G, Tien CL. Partial Coherence Theory of Thin Film Radiative Properties. *Transaction of the ASME:Journal of Heat Transfer.* 1992;114:636-643.
[50] Chen G. Phonon heat conduction in nanostructures. *Int. J. Therm. Sci.* 2000;39:471-480.